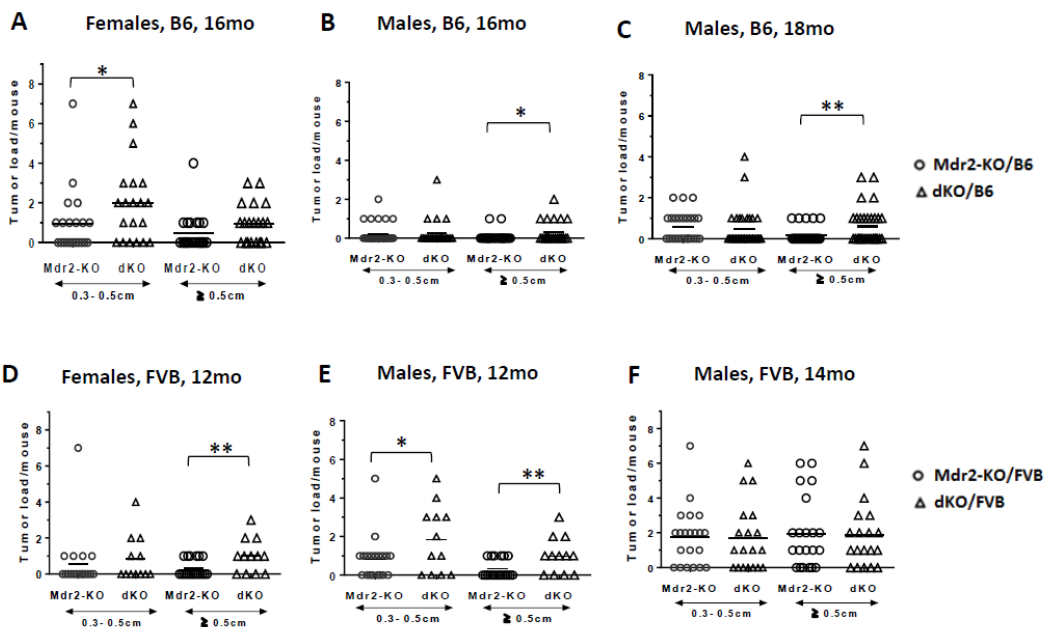
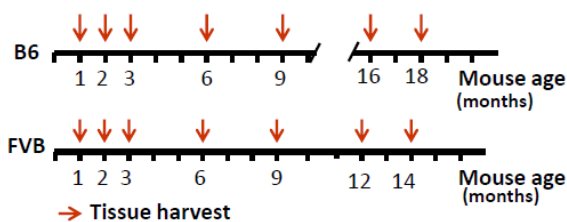
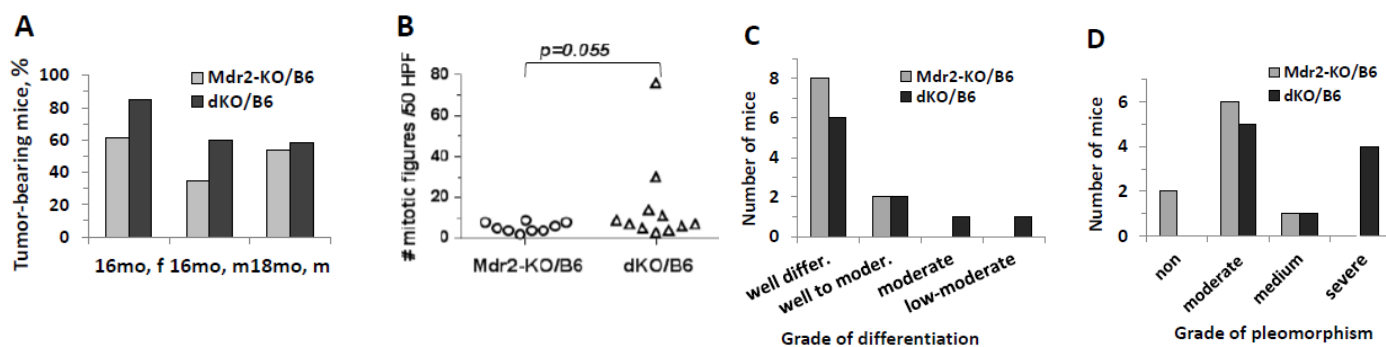


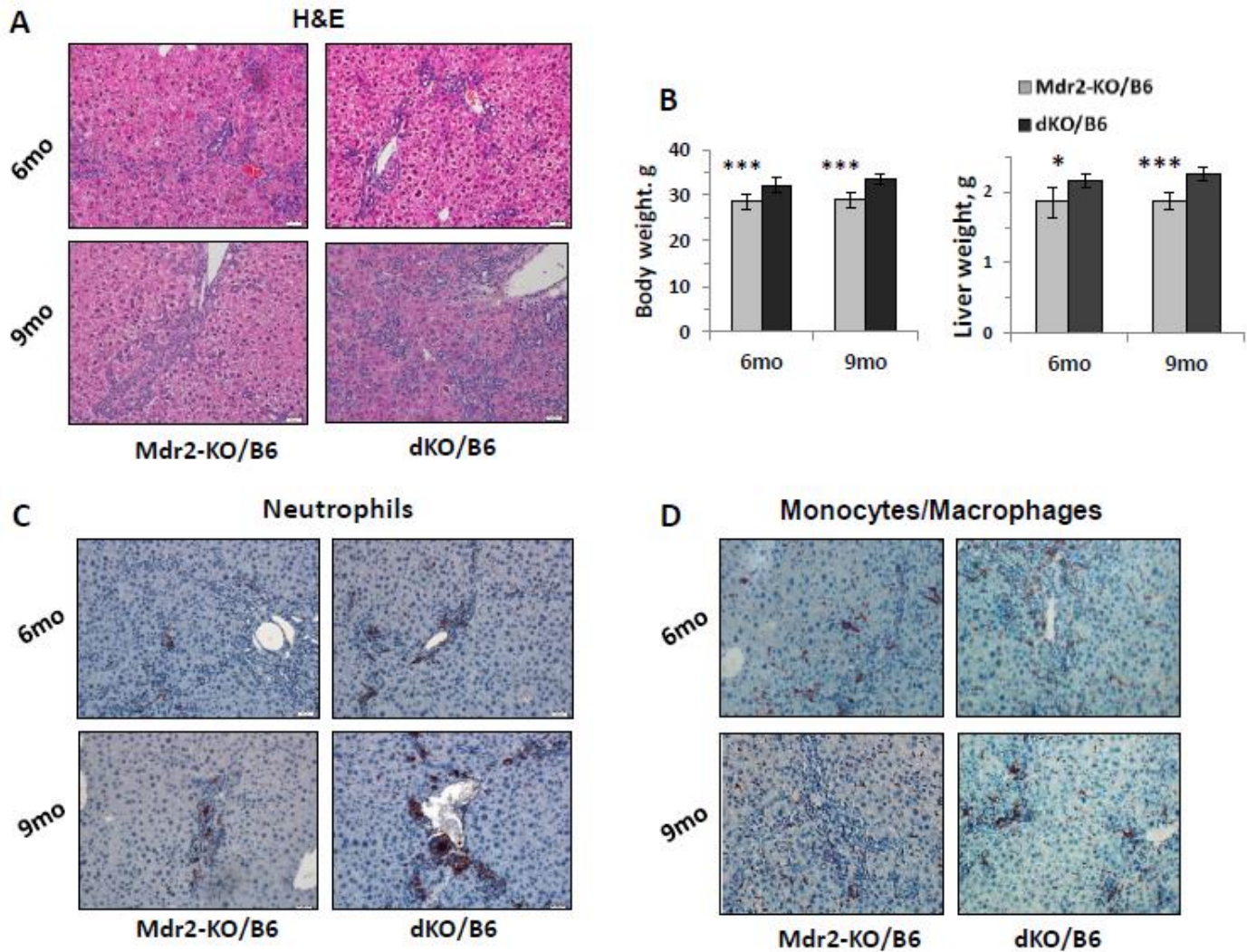
Supplemental Figure S1. Schematic illustration of blood and liver tissue harvest from Mdr2-KO and dKO mice of the B6 and FVB genetic backgrounds.



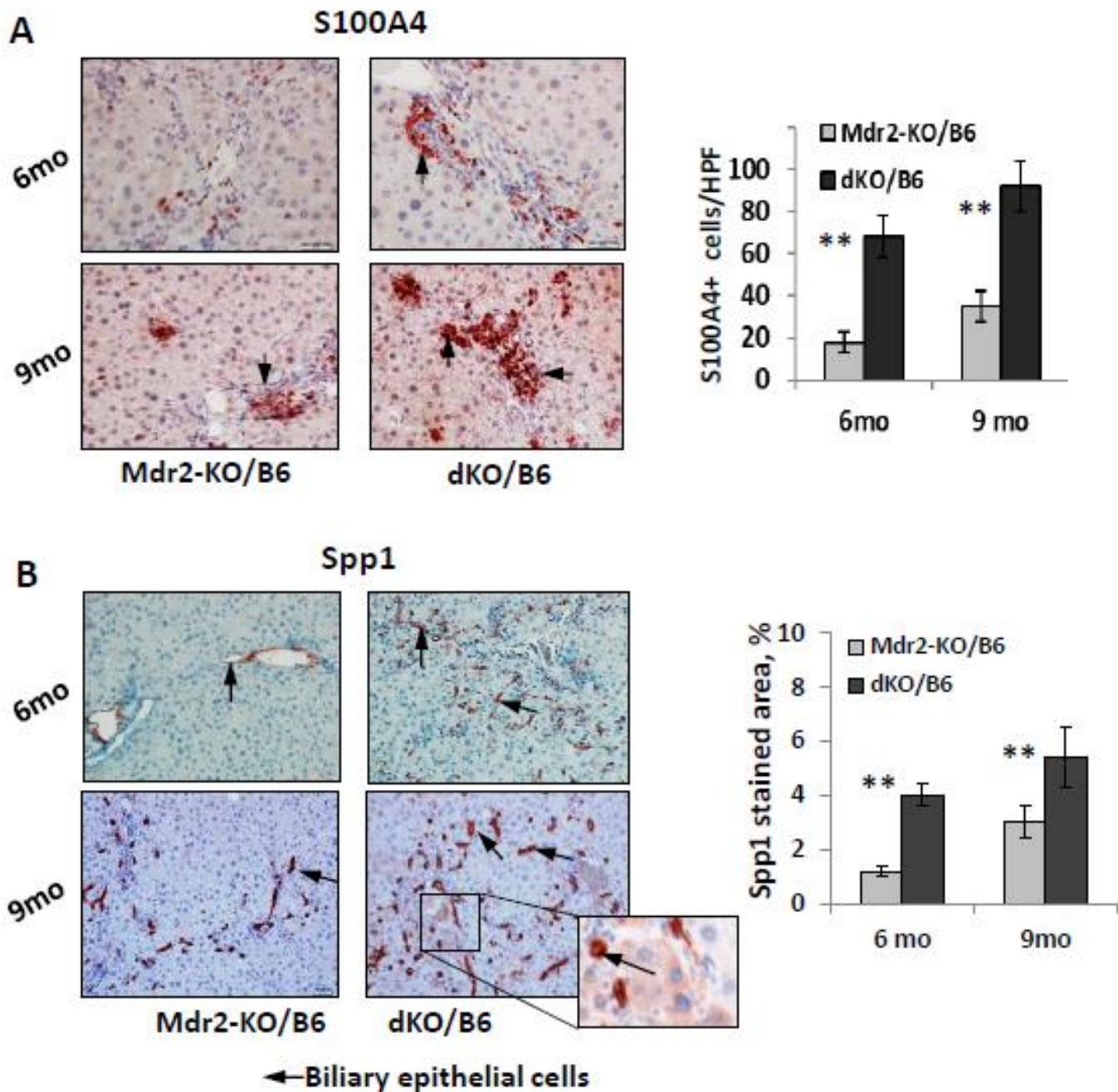
Supplemental Fig. S2. Tumor load in Mdr2-KO and dKO mice. Tumor load per mouse for tumors having diameter either ≥ 0.5 cm, or 0.3-0.49 cm. Tumor load per mouse for the following experimental groups of B6 mice: *A*) 16-month-old females (Mdr2-KO, n=18 and dKO, n=20); *B*) 16-month-old males (Mdr2-KO, n=23 and dKO, n=15); *C*) 18-month-old males (Mdr2-KO, n=26 and dKO, n=29). Tumor load per mouse for the following experimental groups of FVB mice: *D*) 12-month-old females (Mdr2-KO, n=15 and dKO, n=12); *E*) 12-month-old males (Mdr2-KO, n=19 and dKO, n=12); *F*) 14-month-old males (Mdr2-KO, n=15 and dKO, n=12). Only nodules with a diameter ≥ 0.3 cm were calculated. Statistical significance was calculated using two-tailed t-test (#, $P < 0.05$).



Supplemental Figure S3. Loss of Gall1 in Mdr2-KO/B6 mice accelerates HCC development and aggravates histological characteristics of hepatic tumors. *A*) Number of tumor-bearing mice after HCC initiation. Only nodules with a diameter ≥ 0.3 cm were scored. *B*) Number of mitoses in HCC tumors of Mdr2-KO and dKO/B6 mice at 18 month of age. *C*) Mice distribution according to the grade of tumor differentiation. *D*) Mice distribution according to the grade of tumor cell pleomorphism. Histologic characteristics were evaluated in a blind manner by pathologist (O.P.) from H&E-stained liver cuts. Statistical significance (t -test) is indicated: $P=0.055$ in dKO vs Mdr2-KO mice. $N=10$ for Mdr2-KO/B6 and $n=11$ for dKO/B6 males at 18 months of age.

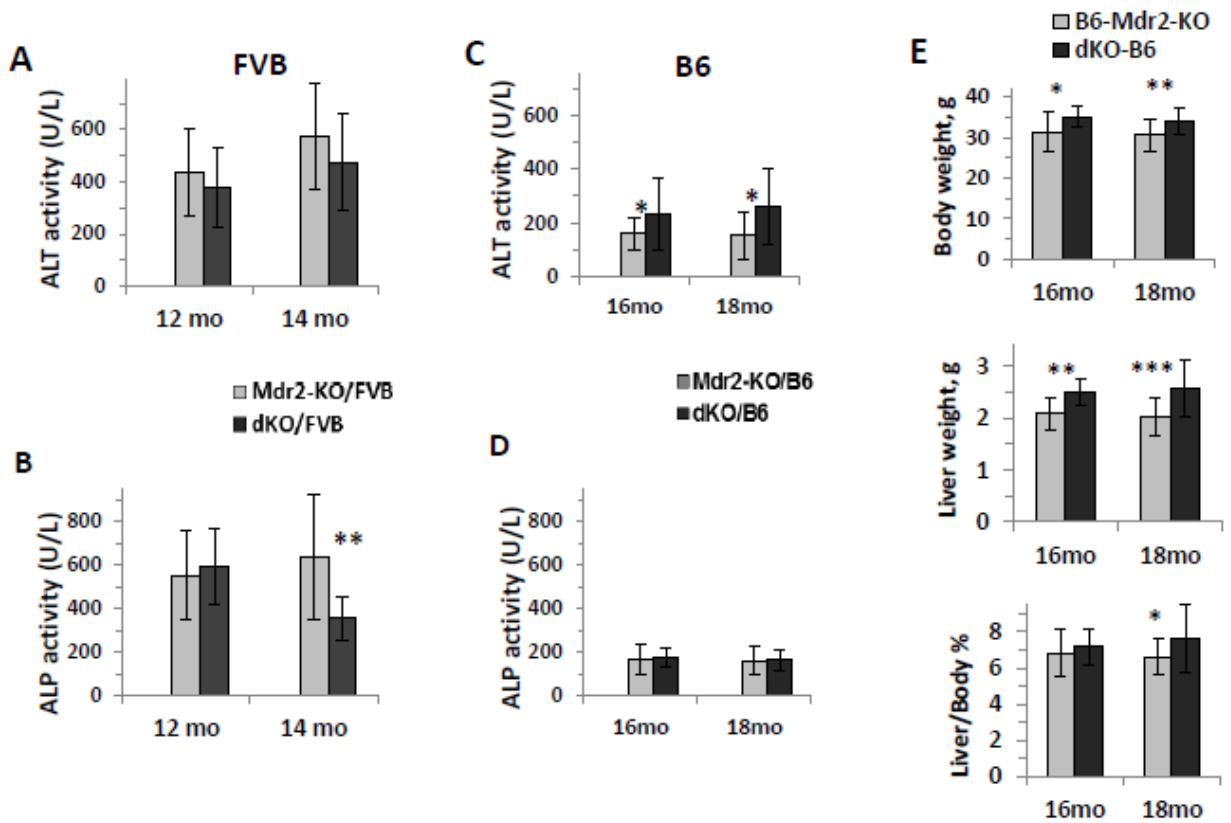


Supplemental Figure S4. Gal1 deficiency exacerbates inflammation and leukocytes recruitment in the livers of middle-aged Mdr2-KO/B6 mice. *A*) H&E histostaining and *B*) body and liver weights of Mdr2-KO/B6 and dKO/B6 males of 6 and 9 month of age. *C*, *D*) Liver tissue sections of Mdr2-KO/B6 and dKO/B6 males aged 6 and 9 months were immunostained with either Ly-6G (*C*) or F4/80 (*D*). Quantification of Ly-6G-positive and F4/80-positive leukocytes – in the Fig. 7B and 7C, respectively. PMN are located in the region of fibrotic septa and biliary reaction. Magnification x200. Four-six males per each experimental group, 10 images were collected and analyzed per each mouse. The values are mean \pm SD. *, $P < 0.05$, **, $P < 0.05$.

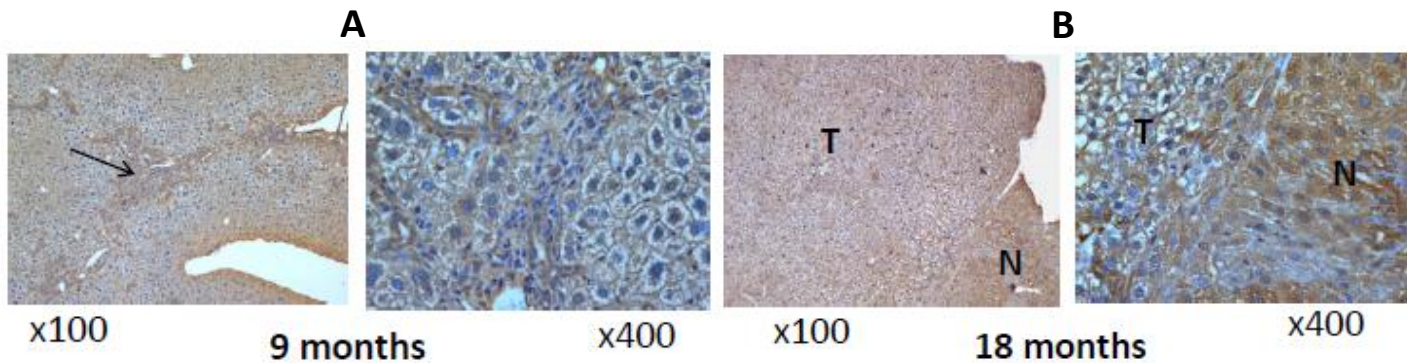


Supplemental Figure S5. Evidence for augmented EMT transition in the livers of middle-aged dKO/B6 mice.

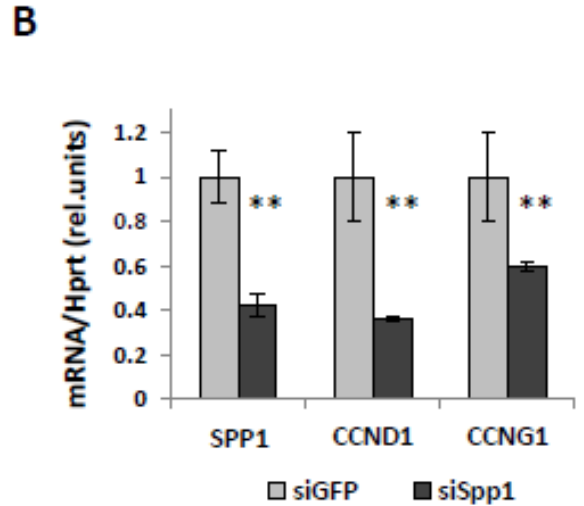
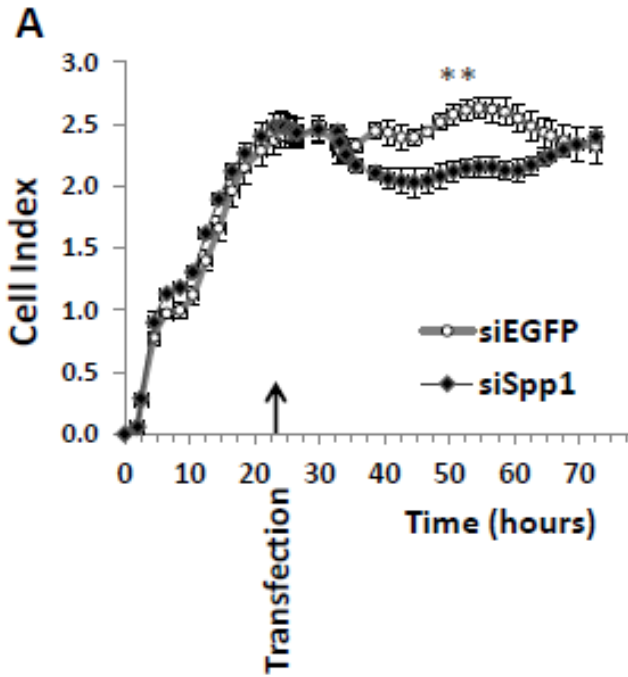
Immunostaining for S100A4 (A) and Spp1 (B) and quantification by morphometric analysis in the livers of Mdr2-KO/B6 & dKO/B6 mice at 6 and 9 months of age. Of note, immunostaining did not detect any S100A4 protein in Mdr2-heterozygous liver (not shown). Magnification x400; scale bar 20 μ M; n=3-5 mice/genotype. The results are shown as means and standard errors of the mean. Statistical significance (*t*-test): **, $P < 0.005$ in dKO vs Mdr2-KO mice.



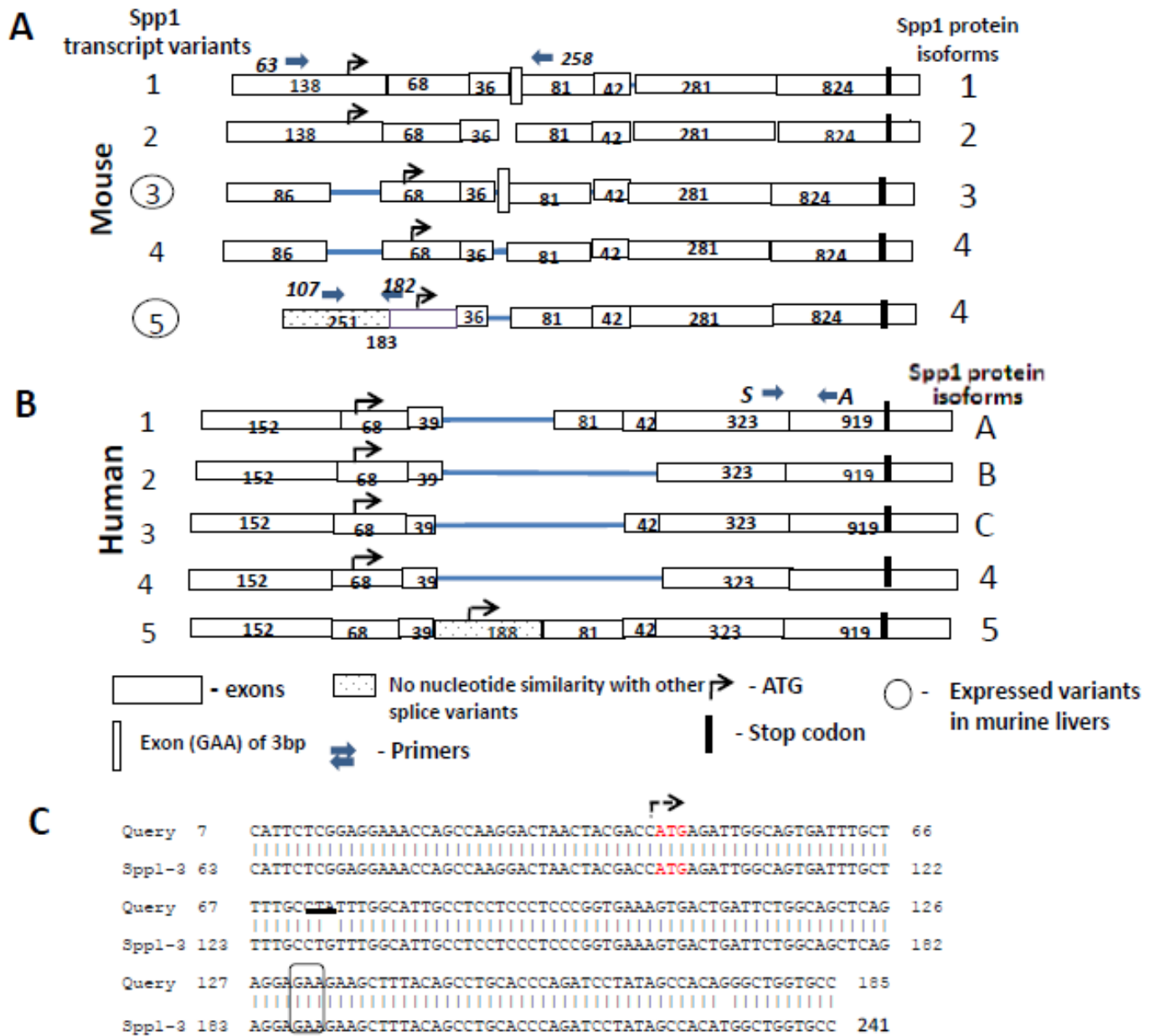
Supplemental Figure S6. Increased inflammation in the livers of aged dKO/B6 vs. Mdr2-KO males. A, B) Serum ALT and ALP activities (units/Liter) from 12- and 14-months-old dKO and Mdr2-KO males of the FVB genetic background. C, D) Serum ALT and ALP activities (units/Liter) from 16- and 18-months-old dKO and Mdr2-KO males of the B6 genetic background. The mouse numbers in each experimental group is as in the Fig. 1. Note that the ALT and ALP values remain much higher in the FVB compared to the B6 congenic mice. E) Body, liver weights and liver/body weight ratio of old males from B6 congenic strains. The results are shown as means \pm SD. Statistical significance (*t*-test): *, $P < 0.05$ and **, $P < 0.005$, ***, $P < 0.0005$ in dKO vs Mdr2-KO mice.



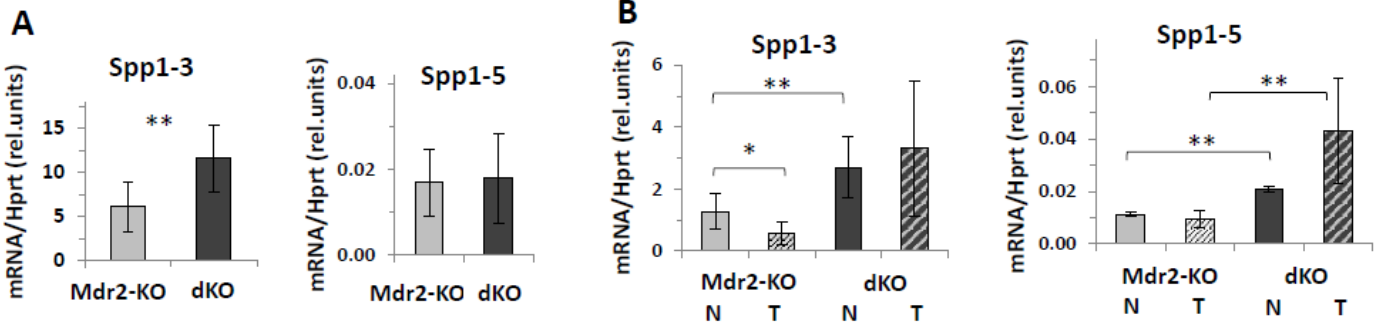
Supplemental Figure S7. Immunohistochemical staining for Gal1 of liver tissue sections from the aged B6 Mdr2-KO mice. Representative images from: A) 9 months old mouse; B) 18 months old mouse. Magnifications x100 and x400. Arrow points to biliary tracts. T - tumor; N - non-tumor liver tissue.



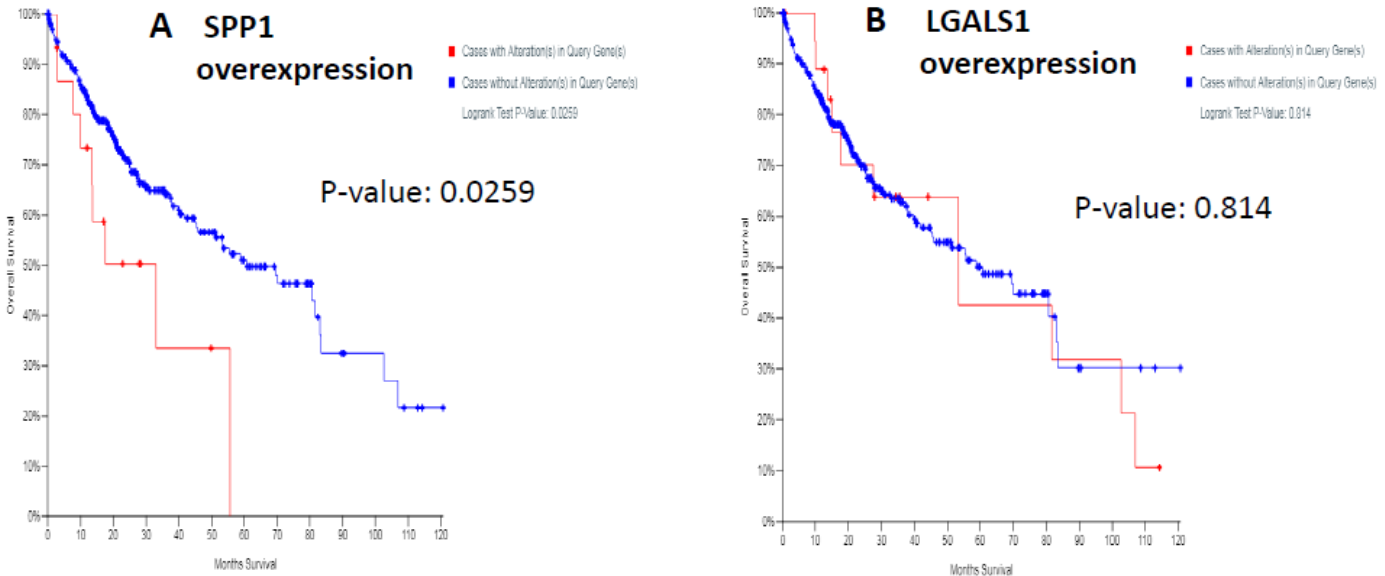
Supplemental Figure S8. SPP1 knockdown in HepG2 cells results in retardation of cell proliferation. *A)* At 24 hours post plating, HepG2 cells were transfected with either siSPP1 or control siGFP. Rate of HepG2 proliferation grown in 16-well plate (analog of 96-well plate) was assigned by real-time xCELLigence technology (Roche Diagnostics). *B)* Real-Time PCR demonstrates reduced expression of SPP1, CCND1 and CCNG1 genes in the tested HepG2 cells at 38 hours after transfection with either siSpp1 or siGFP. Total RNA was extracted from cells grown in the 24-well plates. The results were normalized to the housekeeping HPRT values. The data are expressed as a mean \pm SD mRNA levels for each group (n=3 in each group). **P<0.005 in siSPP1 vs. siGFP group.



Supplemental Figure S9. Schematic structure of murine and human Spp1 gene splicing variants. A) Schematic structure of murine Spp1 transcript splice variants reported in GenBank and primers for them. According to our data only transcript variants 3 and 5 are expressed in Mdr2 congenic livers. Primers 63 and 258 were used to detect presence of Spp1 splice variants 1, 2, 3, 4. Primers 63-258 produce PCR products of 195 or 192 bp, that include or not include the 3-codon exon, for Spp1-1 and Spp1-3 isoforms, respectively. Exon GAA of 3 bp spans nucleotide positions 243-245 or 191-193 in the splice variants 1 or 3, respectively. Primers 107-182 produce PCR product of 76 bp that is specific for Spp1-5 only. B) Schematic structure of human Spp1 transcript splice variants reported in GenBank. Primers *sense* and *antisense* that are common for all 5 splice variants were used for RT-PCR tests of human SPP1 expression. For both diagrams, exons are represented by boxes with a size approximately proportional to their length. Spp1 protein isoforms that are encoded by respective transcript variants are shown at right. C) Spp1 transcript splice variant 3 is expressed in the mouse liver. Alignment of PCR product 63-258 with Spp1-3 transcript. Rectangle marks exon (GAA) of 3 bp only. Silent mutation (CTA, CTG) that encodes L=Leucine is underlined.



Supplemental Figure S10. The expression profile of murine Spp1 splice variants. Only Spp1-3 and Spp1-5 are expressed in B6 livers according to the data of RT-PCR and sequencing. Hepatic Spp1 were PCR-amplified with primers common for splice variants Spp1-1,2,3,4 on RNAs from Mdr2-KO & dKO of 2-month- and 16-month-old mice (T and N). Each murine liver RNA was RT processed and equal cDNA amounts were mixed for the PCR assays. Primers 63 and 258 were used to detect presence of 1, 2, 3, 4 Spp1 splice variants. A) Hepatic expression of Spp1 isoforms in 2-month-old Mdr2-KO/B6 and dKO/B6 mice. B) Hepatic expression of Spp1 isoforms in N and T tissues of 16-month-old Mdr2-KO/B6 & dKO/B6 mice. 4–6 mice for each time point. Standard deviation and statistical significance (*t*-test) are indicated: *, $P < 0.05$ and **, $P < 0.01$.



Supplemental Figure S11. The Kaplan-Meier estimates of overall survival of HCC patients with over-expressed SPP1 or LGALS1 genes. A) Overall survival of patients (360 total) with (14) or without (346) overexpression of SPP1. B) Overall survival of patients (360 total) with (21) or without (339) overexpression of LGALS1. Data from the cBioPortal database. Samples with overexpression of SPP1 or LGALS1 are shown in red.